ENSO and the North Pacific Gyre Oscillation: an integrated view of Pacific decadal dynamics

Di Lorenzo[1*] E., N. Schneider[2] and K. M. Cobb[1], J. C. Furtado[1] and M. A. Alexander[3]

[1] *School of Earth and Atmospheric Sciences, Georgia Institute of Technology, GA*

[2] *International Pacific Research Center, University of Hawaii at Manoa, HI*

[3] *NOAA/Earth System Research Laboratory, Boulder, CO*

submitted to

Geophysical Research Letters

[*]Corresponding Author:

Emanuele Di Lorenzo

School of Earth and Atmospheric Sciences

Georgia Institute of Technology

311 Ferst Drive, Atlanta, GA 30332

Email: edl@gatech.edu

ABSTRACT

We show that decadal dynamics of the Pacific Decadal Oscillation (PDO) and the North Pacific Gyre Oscillation (NPGO) are linked through their relationships to ENSO. The PDO and NPGO are the oceanic expression of the two dominant modes of North Pacific atmospheric variability -- the Aleutian Low (AL) and the North Pacific Oscillation (NPO). We compute the two dominant modes of ocean/atmosphere co-variability in the Pacific sector [40S-62N] and find that the first co-variability mode captures the mature phase of ENSO and its atmospheric teleconnections to the AL, while the second co-variability mode captures the NPGO/NPO tropical expression, which leads the ENSO mode by ~8-12 months. The atmospheric projections of these first two modes are used to extract the AL and NPO forcings related to ENSO. These forcings are then integrated with an AR-1 model and lead to skillful reconstructions of the PDO (R=0.65), NPGO (R=0.60), and Pacific surface temperature decadal variance (R=0.4-0.8). We synthesize these results with previous studies and propose a possible framework for quasi-deterministic decadal oscillations of Pacific climate.

1. Background and Motivation

Low-frequency fluctuations in physical and biological variables in the North Pacific are characterized by two dominant modes of oceanic variability, the Pacific Decadal Oscillation (PDO) [*Mantua et al., 1997; Zhang et al., 1997*] and the more recently recognized North Pacific Gyre Oscillation (NPGO) [*Di Lorenzo et al., 2008, 2009*]. The PDO is defined as the dominant mode of variability of North Pacific sea surface temperature anomalies (SSTa) and is highly correlated with the dominant mode of sea surface height anomalies (SSHa) [*Chhak et al., 2009*]. Its temporal modulations are linked to several biological and ecosystem variables in the ocean [*Hare and Mantua, 2000*]. The NPGO is defined as the second dominant mode of SSHa variability in the Northeast Pacific [180°–110°W; 25°N–62°N] and very closely tracks the second mode of North Pacific SSTa [*Di Lorenzo et al., 2008*]. The NPGO explains the low-frequency fluctuations of upper ocean salinity and nutrients observed in long-term records of the Northeast Pacific, and physically captures changes in strength of the North Pacific Current (NPC) [*Di Lorenzo et al., 2009*] and of the Kuroshio-Oyashio Extension (KOE) [*Ceballos et al., 2009*] .

Dynamically, both the PDO and NPGO are the oceanic expressions of atmospheric variability in the midlatitude Pacific [*Chhak et al., 2009*]. Specifically, the PDO is predominantly driven by variability in the Aleutian Low (AL) -- the first mode of sea level pressure anomaly (SLPa) variability in the North Pacific [*Trenberth and Hurrell, 1995*], while the NPGO is dominantly forced by variability associated with the North Pacific Oscillation (NPO) -- the second mode of North Pacific SLPa [*Walker and Bliss, 1932; Rogers et al., 1981*]. From an atmospheric perspective, both the AL and NPO have been linked to changes in weather patterns over North America, particularly changes in storm tracks, temperatures, and precipitation [*Seager et al., 2005; Linkin and Nigam, 2008; and references therein*].

While the North Pacific decadal variability includes elements independent from the tropics [*Latif and Barnett, 1994; Barnett et al., 1999; Pierce et al., 2001; Liu et al., 2002*], the underlying dynamics responsible for the PDO and NPGO expressions are best understood by considering the role of the tropical Pacific and of the coupling between the tropics and midlatitudes. Several studies have now linked the midlatitude variability of the PDO/AL to ENSO, both statistically and dynamically [*Pierce et al., 2000; Deser et al., 2004; Alexander et al., 2002; 2008; Vimont, 2005; Newman et al. 2003*]. More recent theories have also explored the atmospheric NPO as the driver of SSTa in the central tropical Pacific that favor ENSO by weakening the Walker cell [*Vimont et al., 2003; Anderson et al., 2003*]. These results suggest that the NPGO -- the low-frequency oceanic expression of NPO in the North Pacific -- is also connected to ENSO.

The aim of this paper is to quantify the decadal-scale dynamics of the Pacific and explore a unified conceptual framework of Pacific climate variability that relies on the connections between ocean decadal variations (e.g. PDO, NPGO), their atmospheric forcings (e.g. AL, NPO), and the ENSO cycle. We extract the AL and NPO variability that is linked to the ENSO cycle by computing the two dominant modes of ocean/atmosphere co-variability in the Pacific sector [40S-62N] (section 2-3). We show that using these forcing functions in a simple AR-1 model leads to significant skill in reconstructing the PDO (R=0.65), NPGO (R=0.60), and Pacific SSTa (R=0.4-0.8) (section 4). Finally, we discuss a dynamical framework that may form the physical basis for quasi-deterministic low frequency oscillations in both physical and biological variables of the Pacific Ocean (section 5).

2. Data and Methods

We use monthly sea level pressure anomalies (SLPa) from the National Centers for Environmental Prediction / National Center for Atmospheric Research (NCEP/NCAR) Reanalysis Project [*Kistler et al., 2001*] and SSTa from the National Oceanic and Atmospheric Administration (NOAA) Extended Reconstruction SSTs (NOAA ER SSTs) [*Smith and Reynolds, 2004*] from 1950 to 2006 over 40°S-62°N, 150°E-65°W.

To extract the modes of co-variability of the ocean and atmosphere in the Pacific Ocean, we use a simultaneous Empirical Orthogonal Functions (EOFs) of the SLPa and SSTa fields, referred here as SEOF. In SEOFs, two or more data fields are put into one large space and time matrix that is consequently decomposed via singular value decomposition. Prior to computing the SEOFs, the SSTa is normalized by the domain average standard deviation and the SLPa normalized along each latitude by the standard deviation at that latitude. The data are smoothed in time using a 4-month running mean.

3. Ocean and Atmosphere co-variability in the Pacific Ocean

The two leading modes of ocean/atmosphere co-variability over the Pacific basin extracted from the simultaneous EOF analysis of the SLPa/SSTa are presented in Figure 1. Each mode is characterized by an atmospheric spatial pattern (SEOF SLPa), an ocean pattern (SEOF SSTa) and a Principal Component (PC) timeseries that shows how these patterns evolve through time.

The first ocean/atmosphere co-variability mode (Figure 1, left column) displays the canonical ENSO horseshoe pattern in the SSTa SEOF1 field, with warming in the cold tongue region over the eastern tropical Pacific flanked by cold anomalies in the western Pacific Ocean. The corresponding SLPa SEOF1 field displays both a weaker Walker circulation in the tropics with higher pressure over the western tropical Pacific, as well as a deepening and a southward shift of the Aleutian Low in the North Pacific. The temporal evolution of this pattern (PC1) is highly correlated with the Niño3.4 index (R=0.86). We refer to this as the "ENSO mode".

The second ocean/atmosphere co-variability mode (Figure 1, right column) reveals the typical signature of the NPO in the atmospheric SLPa SEOF2, with the two loading centers over Hawaii and the Aleutian Islands. This pattern is very similar to that reported in previous studies of the NPO [*Walker and Bliss, 1932; Rogers, 1981; Vimont et al., 2003; Linkin and Nigam, 2008*]. The corresponding ocean mode in SSTa SEOF2 exhibits a region of negative SST anomalies in the western and central North Pacific, encircled by warm anomalies extending from the central Gulf of Alaska, down the North American coast, and into the central tropical Pacific. In the midlatitude and the North Pacific, the spatial pattern of the SSTa SEOF2 is nearly identical to the SSTa expression of the NPGO and of the second EOF of North Pacific SSTa, which is has been referred to as the Victoria Mode [*Bond et al., 2003*]. This is also evident from the significant correlation between the temporal evolution of PC2 with the NPGO index (R=0.44; > 95%). We refer to this as the "NPGO/NPO mode".

In the tropical/subtropical latitudes [20S-20N], we note the SSTa SEOF2 is characterized by warm anomalies in the central tropical Pacific and cold anomalies to the east and west, particularly along the South American coast. This SSTa pattern in the tropics is essentially the same as the one isolated by other studies as an ENSO SSTa precursor or as the El Niño Modoki introduced by T. Yamagata [*Ashok et al., 2007*]. Statistical [*Emery and Hamilton, 1985; Penland et al., 1993; Penland and Sardeshmukh, 1995;* Trans-Niño Index (TNI) *Trenberth and Stepaniak, 2001; Anderson et al. 2003*] and dynamical analysis [e.g. the Seasonal Footprinting Mechanism (SFM) by *Vimont et al., 2003;* Meridional Mode (MM), *Chiang and Vimont, 2004; Chang et al.,* *2007*] show that this SSTa pattern leads the mature ENSO anomalies by about ~8-12 months. We confirm this result by exploring the temporal lead/lag relationship between the PC1 (ENSO) and PC2 (NPGO/NPO) inferred from the simultaneous EOFs of SLPa/SSTa. Figure 2a shows that the timeseries of PC1 (ENSO) is significantly correlated with PC2 (NPGO/NPO) (R=0.6; > 97%) when PC2 leads by ~12 months. This 12-month lag emerges from the temporal lagged cross-correlation function between PC1 (ENSO) and PC2 (NPGO/NPO) (Figure 2b).

4. Forced Decadal Dynamics and ENSO

Previous studies have shown that the decadal variations of the PDO and NPGO emerge from integrating the atmospheric forcing of the AL [*Schneider and Cornuelle, 2006*] and NPO [*Chhak et al., 2009*]. We define the indices AL_{rec} and NPO_{rec} as the atmospheric SLPa projections of the first two co-variability modes (Figure 3a,b), and use them as proxies of the AL and NPO atmospheric forcings related to ENSO. Similar to Newman et al. [*2003*] we then quantify the fraction of variability of the PDO and NPGO that is forced by the AL_{rec} and NPO_{rec} by solving a simple one dimensional AR-1 model:

$$\frac{dPDO_{rec}}{dt} = AL_{rec}(t) - \frac{PDO_{rec}}{\tau_{PDO}}$$
$$\frac{dNPGO_{rec}}{dt} = NPO_{rec}(t) - \frac{NPGO_{rec}}{\tau_{NPGO}}$$

where τ_{PDO} = 5 month is the damping timescale/memory of the PDO [*Schneider and Cornuelle, 2006*] and τ_{NPGO} = 10 months [*Chhak et al., 2009*]. The reconstructed indices are significantly correlated with the PDO (R=0.65) and NPGO (R=0.6) indices (Figure 3a,b) . These correlations are higher on ENSO (2-7 years) and low-frequency (>7 years) timescales (R~0.75-0.85). Given the connections of the AL_{rec} and NPO_{rec} forcings to the ENSO cycle these results imply that the two dominant modes of ocean and atmosphere decadal variability, namely the PDO/AL and the NPGO/NPO, are physically linked. Consistent with this view, the lagged cross-correlation function between the timeseries of PC1 and PC2 of North Pacific SLPa, which are typically used to isolate and define the the AL and NPO modes [*Linkin and Nigam, 2008*], exhibit a lead/lag relationship similar to the one obtained between the SEOF1 (ENSO mode) and SEOF2 (NPGO/ NPO mode) (Figure 2b, gray line).

We also quantify the forced decadal dynamics of the Pacific SSTa associated with PDO and NPGO by considering the same AR-1 model forced by both the AL_{rec} and NPO_{rec}

$$\frac{dSSTa_i}{dt} = \alpha_i \cdot AL_{rec}(t) + \beta_i \cdot NPO_{rec}(t) - \frac{SSTa_i}{\tau_i}$$

and integrated at each spatial location i. The coefficients $\alpha_i, \beta_i, \tau_i$ are determined at each location using a least-square fit. The AR-1 reconstruction has high skill in capturing the decadal (timescales > 7 years) variance of Pacific SSTa (R=0.4-0.8) (Figure 3c). The skill of the reconstructed SSTa in the ENSO frequencies (defined here as 2-7 years) is uniformly high, extending into the tropical Indian and Atlantic oceans (Figure 3d), while timescales < 2 years exhibit reduced skill. (Figure 3e). This AR-1 modeling approach can be generalized to quantify the variance of any physical or biological ocean variable linked to the forcing decadal dynamics of the PDO and NPGO connected to ENSO.

5. AN INTEGRATED VIEW OF PACIFIC DECADAL VARIABILITY

Based on these results and the cited literature we propose the following synthesis of Pacific decadal variability (Figure 4, schematic), where the forced decadal dynamics of the PDO (Figure 4, red path) and NPGO (Figure 4, blue path), are physically linked and connected to tropical variability through the ENSO dynamics. Both the PDO and NPGO are the oceanic expressions of the atmospheric forcing associated with the AL and NPO variability, which are linked to the different phases of the ENSO cycle (Figure 4, schematic). Specifically, the boreal spring variability of the NPO drives SSTa in the central tropical Pacific that initiate the ENSO expression that peaks in the following winter [e.g. the Seasonal Footprinting Mechanism (SFM) by *Vimont et al., 2003; Anderson et al.* 2003]. The peak of ENSO in the following winter excites variability in the AL through well known atmospheric teleconnections [*Alexander, 1992; Alexander et al., 2002*]. The atmospheric teleconnected variability of the AL is integrated and low-passed by the ocean into the PDO pattern [*Newman et al., 2003*] in the same way as the NPO variability is integrated into the oceanic NPGO pattern [*Chhak et al., 2009*].

The oceanic adjustment to the SSHa anomalies of the PDO and NPGO radiate Rossby waves that propagate the signals into the Kuroshio-Oyashio extension region (KOE). The arrival of the PDO SSHa are associated with changes in the axis of the KOE [*Miller and Schneider, 2000; Qiu et al., 2007*], while the NPGO SSHa modulate variations in the speed of the KOE [*Ceballos et al., 2009*] (Figure 4). These two modes of KOE variability, the KOE meridional mode (shift in axis) and the KOE Zonal mode (change in speed), respectively, have been shown to capture the first two modes of variability of SSHa in the KOE [*Taguchi et al., 2007*].

The forcing dynamics of the NPO and its relationship to the tropics require further investigation. Although there are physically-based hypotheses that link the NPO forcing to the

ENSO dynamics [*e.g. the SSTa footprinting mechanism, Vimont et al., 2003;* Meridional Mode (MM), *Chiang and Vimont, 2004; Chang et al., 2007*] and to tropical SSTa [*Vimont et al., 2009*], the source of NPO variability has so far been attributed to intrinsic atmospheric variability in the midlatitudes associated with changes in strength of the storm tracks [*Linkin and Nigam, 2008*]. However, some studies [*Anderson, 2004; 2007*] suggest that part of the NPO variability may not be independent of ENSO and may originate in the equatorial Pacific. If this link is confirmed (Figure 4, gray path), the schematic framework proposed in this study may provide the physical basis for sustained oscillations in the Pacific Ocean. As these dynamics are investigated further in coupled climate models and observations, it will be essential to quantify the role of atmospheric noise in interrupting or exciting some of the dynamical pathways linking the tropics and extra-tropics.

ACKNOWLEDGMENTS

We acknowledge the support of the NSF OCE-0550266 NSF CCE-LTER NSF-GLOBEC OCE-0815280, NASA NNG05GC98G, NSF OCE05-50233 and NSF OCE06-47994, Department of Energy, Office of Science (BER), grant DE-FG02-07ER64469, and NASA, NOAA and JAMSTEC for research support at the IPRC.

REFERENCES

Alexander, M. A. (1992), MIDLATITUDE ATMOSPHERE OCEAN INTERACTION DURING EL NINO .1. THE NORTH PACIFIC-OCEAN, *Journal of Climate*, *5*(9), 944-958.

Alexander, M. A., et al. (2002), The atmospheric bridge: The influence of ENSO teleconnections on air-sea interaction over the global oceans, *Journal of Climate*, *15*(16), 2205-2231.

Alexander, M. A., et al. (2008), Forecasting Pacific SSTs: Linear inverse model predictions of the PDO, *Journal of Climate*, *21*(2), 385-402.

Anderson, B. T. (2003), Tropical Pacific sea-surface temperatures and preceding sea level pressure anomalies in the subtropical North Pacific, *J. Geophys. Res.-Atmos.*, *108*(D23), 18.

Ashok, K., et al. (2007), El Nino Modoki and its possible teleconnection, J. Geophys. Res.-Oceans, 112(C11), 27.

Bond, N. A., et al. (2003), Recent shifts in the state of the North Pacific, *Geophys. Res. Lett.*, *30*(23), 4.

Ceballos, L. I., et al. (2009), North Pacific Gyre Oscillation synchronizes climate fluctuations in the eastern and western boundary systems , Journal of Climate(in press).

Chang, P., et al. (2007), Pacific meridional mode and El Nino-southern oscillation, *Geophys. Res. Lett.*, *34*(16), 5.

Chhak, K., et al. (2009), Forcing of low-frequency ocean variability in the Northeast Pacific, *Journal of Climate*, *22*(5), 1255-1276.

Chiang, J. C. H., and D. J. Vimont (2004), Analogous Pacific and Atlantic meridional modes of tropical atmosphere-ocean variability, *Journal of Climate*, *17*(21), 4143-4158.

Deser, C., A. S. Phillips, and J. W. Hurrell (2004): Pacific interdecadal climate variability: Linkages between the tropics and North Pacific during boreal winter since 1900. *J. Climate*, 17, 3109-3124.

Di Lorenzo, E., et al. (2008), North Pacific Gyre Oscillation links ocean climate and ecosystem change, *Geophys. Res. Lett.*, *35*(8), 6.

Emery, W. J., and K. Hamilton (1985), ATMOSPHERIC FORCING OF INTERANNUAL VARIABILITY IN THE NORTHEAST PACIFIC-OCEAN - CONNECTIONS WITH EL-NINO, J. *Geophys. Res.-Oceans, 90*(NC1), 857-868.

Hare, S. R., and N. J. Mantua (2000), Empirical evidence for North Pacific regime shifts in 1977 and 1989, *Prog. Oceanogr., 47*(2-4), 103-145.

Kistler, R., et al. (2001), The NCEP-NCAR 50-year reanalysis: Monthly means CD-ROM and documentation, *Bull. Amer. Meteorol. Soc.*, *82*(2), 247-267.

Kwon, Y. O., and C. Deser (2007), North Pacific decadal variability in the Community Climate System Model version 2, *Journal of Climate*, *20*(11), 2416-2433.

Linkin, M. E., and S. Nigam (2008), The north pacific oscillation-west Pacific teleconnection pattern: Mature-phase structure and winter impacts, *Journal of Climate*, *21*(9), 1979-1997.

Mantua, N. J., et al. (1997), A Pacific interdecadal climate oscillation with impacts on salmon production, *Bull. Amer. Meteorol. Soc.*, *78*(6), 1069-1079.

Miller, A. J., and N. Schneider (2000), Interdecadal climate regime dynamics in the North Pacific Ocean: theories, observations and ecosystem impacts, *Prog. Oceanogr.*, *47*(2-4), 355-379.

Newman, M., et al. (2003), ENSO-forced variability of the Pacific decadal oscillation, *Journal of Climate*, *16*(23), 3853-3857.

Penland, C., and T. Magorian (1993), PREDICTION OF NINO-3 SEA-SURFACE TEMPERATURES USING LINEAR INVERSE MODELING, *Journal of Climate*, *6*(6), 1067-1076.

Qiu, B., et al. (2007), Coupled decadal variability in the North Pacific: An observationally constrained idealized model, *Journal of Climate*, *20*(14), 3602-3620.

Rogers, J. C. (1981), The North Pacific Oscillation, *J. Climatol.*, *1*, 39-57.

Schneider, N., and B. D. Cornuelle (2005), The forcing of the Pacific decadal oscillation, *Journal of Climate*, *18*(21), 4355-4373.

Seager, R., et al. (2005), Mechanisms of ENSO-forcing of hemispherically symmetric precipitation variability, *Q. J. R. Meteorol. Soc.*, *131*(608), 1501-1527.

Smith, T. M., and R. W. Reynolds (2004), Improved extended reconstruction of SST (1854-1997), *Journal of Climate*, *17*(12), 2466-2477.

Taguchi, B., et al. (2007), Decadal variability of the Kuroshio Extension: Observations and an eddy-resolving model hindcast, *Journal of Climate*, *20*(11), 2357-2377.

Trenberth, K. E., and J. W. Hurrell (1995), *Decadal climate variations in the Pacific*, National Research Council, Natural Climate Variability on Decade-to-Century Time Scales. National Academy Press, Washington, D.C., 472-481.

Trenberth, K. E., and D. P. Tepaniak (2001), Indices of El Nino evolution, *Journal of Climate*, *14*(8), 1697-1701.

Vimont, D. J. (2005), The contribution of the interannual ENSO cycle to the spatial pattern of decadal ENSO-like variability, *Journal of Climate*, *18*(12), 2080-2092.

Vimont, D. J., et al. (2009), Midlatitude Excitation of Tropical Variability in the Pacific: The Role of Thermodynamic Coupling and Seasonality, *Journal of Climate*, *22*(3), 518-534.

Vimont, D. J., et al. (2003), The seasonal footprinting mechanism in the Pacific: Implications for ENSO, *Journal of Climate*, *16*(16), 2668-2675.

Walker, G. T., and E. W. Bliss (1932), World Weather V, *Mem. R. Meteorol. Soc.*, *4*, 53-84.

Zhang, Y., et al. (1997), ENSO-like interdecadal variability: 1900-93, J. Clim., 10(5), 1004-1020.

Figure 1: 1st (*left panels*) and 2nd (*right panels*) co-variability mode of SLPa and SSTa extracted from simultaneous EOF analysis. Each mode is characterized by an expression in SLPa, SSTa, and and a principal component (PC) timeseries that shows how these patterns are modulated in time. The PC1 (ENSO mode) and PC2 (NPGO/NPO modes) are significantly > 95% correlated to the Niño 3.4 (R=0.86) and NPGO (R=0.44) indices respectively. std=units of standard deviation.

Figure 2: (**A**) Correlation of PC1 (ENSO mode) with PC2 (NPGO/NPO modes) leading by 12 months. (B) Temporal lagged cross-correlation function between PC1 (ENSO) and PC2 (NPGO/NPO) (black line), same for the 3 year lowpass AL and NPO indices (gray line).

Figure 3: (*Right panels*) Reconstruction of AL_{rec} (red; **A**) and NPO_{rec} (blue; **B**) atmospheric indices connected to ENSO cycle. PDO_{rec} and $NPGO_{rec}$ are obtained by integrating AL_{rec} and NPO_{rec} with the AR-1 model. Correlations (R) with the true indices are all significants > 95%. Units are in standard deviations (std). (*Right panels*) Global SSTa reconstruction skill of AR-1 model forced with the AL_{rec} and NPO_{rec} components connected to ENSO cycle. Maps show grid point correlation between SSTa reconstruction and observations. (**C**) Correlation of 7 year lowpass timeseries, (**D**) for 2-7 year bandpass and (**E**) 2 year highpass.

Figure 4: Synthesis schematic of Pacific decadal variability (see text in discussion). (Red path) PDO/AL dynamics. (Blue path) NPGO/NPO dynamics.

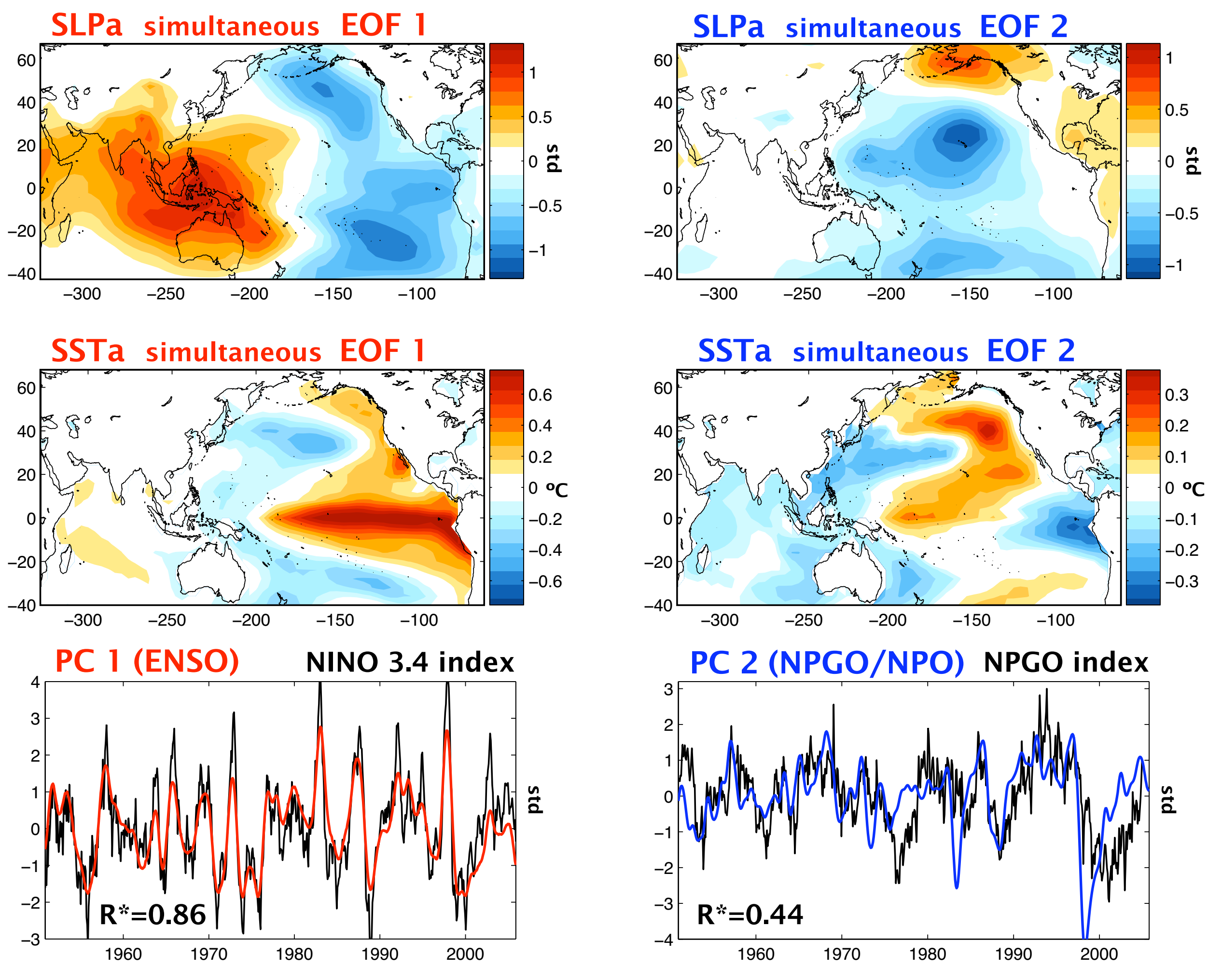

Figure 1: 1st (*left panels*) and 2nd (*right panels*) co-variability mode of SLPa and SSTa extracted from combined EOF analysis. Each mode is characterized by an expression in SLPa, SSTa, and and a principal component (PC) timeseries that shows how these patterns are modulated in time. The PC1 (ENSO mode) and PC2 (NPGO/NPO modes) are significantly > 95% correlated to the Niño 3.4 (R=0.86) and NPGO (R=0.44) indices respectively. std=units of standard deviation.

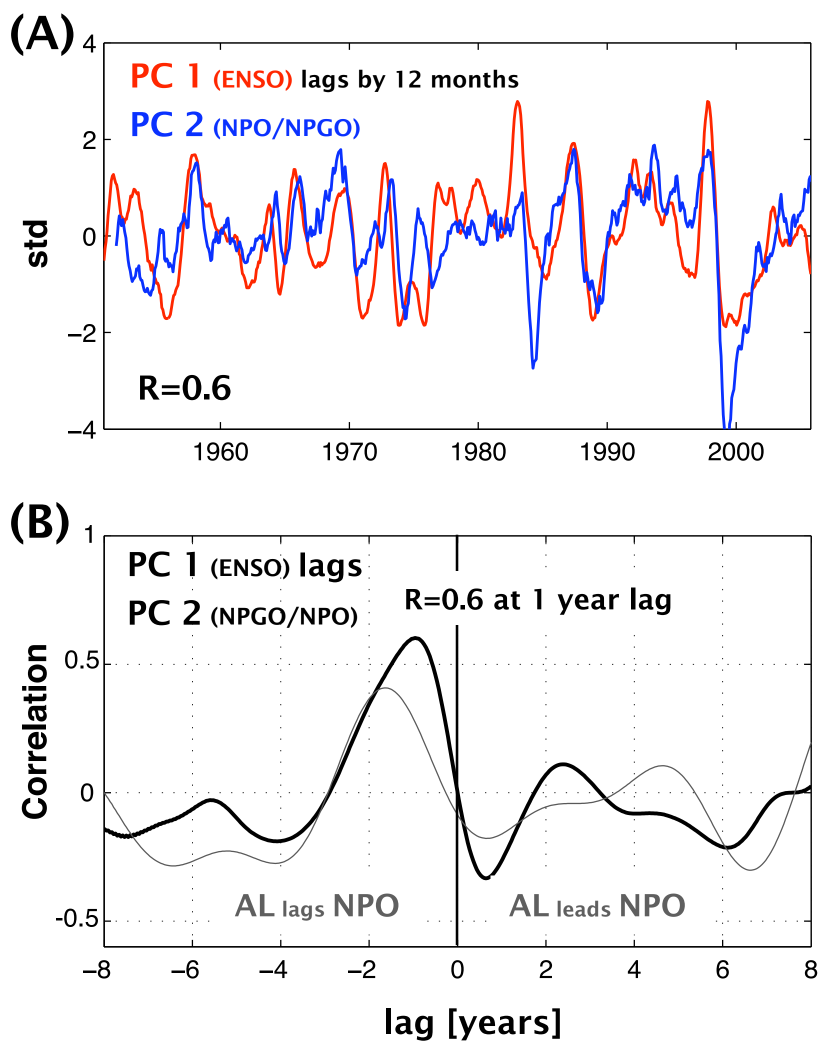

Figure 2: (**A**) Correlation of PC1 (ENSO mode) with PC2 (NPGO/NPO modes) leading by 12 months. (B) Temporal lagged cross-correlation function between PC1 (ENSO) and PC2 (NPGO/NPO) (black line), same for 3 year lowpass AL and NPO indices (gray line).

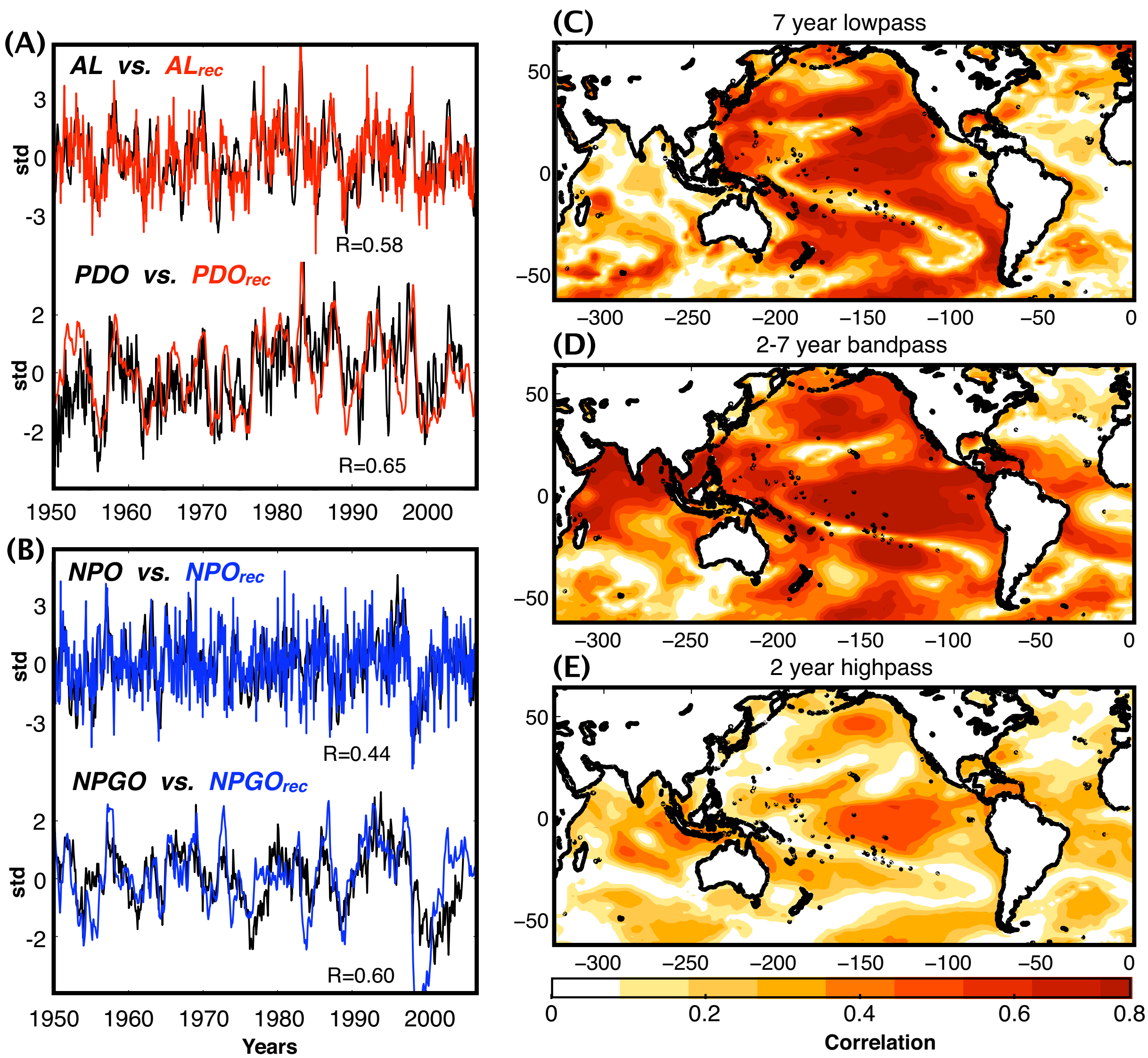

Figure 3: (*Right panels*) Reconstruction of AL_{rec} (red; **A**) and NPO_{rec} (blue; **B**) atmospheric indices connected to ENSO cycle. PDO_{rec} and $NPGO_{rec}$ are obtained by integrating AL_{rec} and NPO_{rec} with the AR-1 model. Correlations (R) with the true indices are all significants > 95%. Units are in standard deviations (std). (*Right panels*) Global SSTa reconstruction skill of AR-1 model forced with the AL_{rec} and NPO_{rec} components connected to ENSO cycle. Maps show grid point correlation between SSTa reconstruction and observations. (**C**) Correlation of 7 year lowpass timeseries, (**D**) for 2-7 year bandpass and (**E**) 2 year highpass.

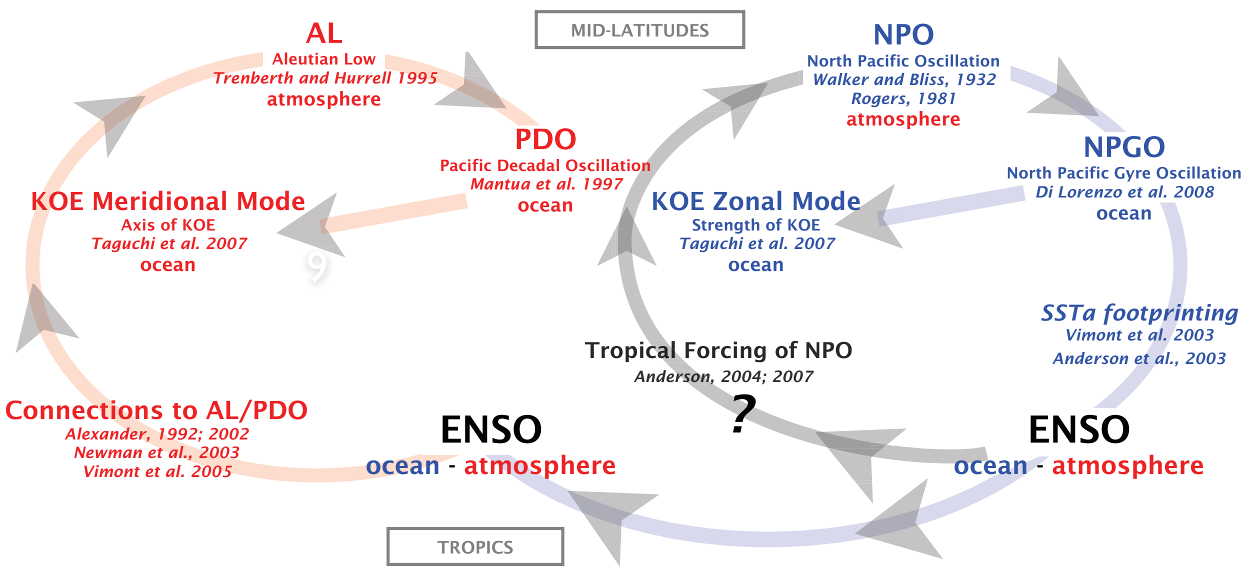

Figure 4: Synthesis schematic of Pacific decadal variability (see text in discussion). (Red path) PDO/AL dynamics. (Blue path) NPGO/NPO dynamics.